# Optimal Planning of Single-Port and Multi-Port Charging Stations for Electric Vehicles in Medium Voltage Distribution Networks

Biswarup Mukherjee, *Member, IEEE,* and Fabrizio Sossan, *Member, IEEE*

*Abstract*—This paper describes a method to cost-optimally locate and size chargers for electric vehicles (EVs) in power distribution grids as a function of the driving demand while respecting the grid's constraints. The problem accounts for the notion of single-port chargers (SPCs), where a charger can interface one EV maximum, and multi-port chargers (MPCs), where the same charger can interface multiple EVs, leading to possible cost savings and improved arbitrage of the charging power. The formulation is capable of accounting for and modeling the flexibility of EV owners' in plugging and unplugging their EVs from and to chargers at different hours of the day, a factor that can impact chargers' utilization and thus charging infrastructure requirements. Simulation results from a synthetic case study show that implementing MPCs is cost-beneficial over both SPCs and owners' flexibility for EVs with small batteries (16 kWh). However, this cost benefit vanishes when considering EVs with larger batteries (60 kWh).

*Index Terms*—EVs; Charging stations; Distribution networks; Optimal power flow; single-port chargers; multi-port chargers.

## I. INTRODUCTION

The massive adoption of electric vehicles (EVs) will play a central role in decarbonizing road transportation [1]–[4]. Recharging EVs requires to develop an extended and pervasive charging infrastructure. Reference [5] estimates that, between 2019-2025, more than 2 billion Dollars will be necessary to improve the public and residential charging infrastructure across major U.S. metropolitan areas, whereas, in France, 2 billion Euros will be required to achieve the target of 7 million deployed public and private chargers by 2030 [3], [6]. In addition to these investments, others will be necessary to adapt the electrical grid infrastructure, in particular distribution grids. Indeed, it is well known that the connection of many chargers in distribution grids might lead to congesting substation transformers and power lines and to violations of statutory voltage limits (e.g., [7], [8]). This is because distribution grids were designed to host prescribed amounts of demand and with predefined voltage gradients on the feeders, which are altered when massively recharging EVs. The large investments required to both install suitable charging infrastructure for EVs and upgrade existing distribution networks motivate the need

Both authors are with the Centre for processes, renewable energies and energy systems (PERSEE) of MINES ParisTech - PSL University, France. E-mail: biswarup.mukherjee, fabrizio.sossan@minesparis.psl.eu

to research formal methods to locate and size EV chargers accounting for realistic driving demand patterns, technical limits of existing distribution grids, and the cost of the chargers.

In this context, this paper proposes a method to locate and size EV chargers accounting for the driving demand and the constraints of existing distribution grids. The method can model different types of chargers, such as fast and slow chargers, as well as single-port chargers (SPCs) and multi-port chargers (MPCs). In addition, it can model the availability of the EV owners to plug and unplug EVs to and from public charging stations, an element that can achieve better utilization of the charging columns, thus impacting the number of chargers to deploy. The method is thought for an integrated distribution system operator (DSO)/urban planner willing to estimate a cost-optimal charging infrastructure while accounting for the technical limitations of the grid, different types of chargers, and EV owners' behaviors.

The problem of planning the EVs recharging infrastructure is not new and has been extensively investigated in the literature, although not in the terms proposed in this paper, as it will be now discussed. A multi-objective planning model for laying out EV charging stations is proposed in [9], without considering, however, the distribution grid's operational constraints. The work in [10] proposes joint planning of EVs charging stations and distribution capacity expansion, without modeling, however, MPCs and EV owners' flexibility. Authors of [11] proposed a method for the cost-optimal planning of EV charging stations in a distribution grid considering grid constraints; however, this work did not consider MPCs that, as shown in this paper, can lead to different EV chargers configurations. Optimal planning of charging stations was also developed in [12], [13], without however including grid constraints. The work in [14] proposes a planning method for MPC chargers considering a parking slot; we extend this notion to a whole distribution grid. In [15], and similarly in [16], both power flows in a power distribution grid and traffic flows in a transportation network were used to identify appropriate nodes to locate and size the EV charging stations. This work uses a genetic algorithm to solve nonconvex AC load flows, a formulation that could not scale well to a large number of EVs, and does not consider voltage and line ampacities constraints, only the rated power of the nodes. The work in [17] proposes a data-driven approach for identifying driving demand and, based on this information, advises system planners on suitable locations for the charging infrastructure without considering, however, grid constraints. More recently,

the work in [18], [19] proposed a two-stage optimization framework to co-optimize the design and operations of EV charging, power grid, and gas network. This work does not include multi-port chargers and EV owners' flexibility.

In the light of the current state-of-the-art, the main contribution of this paper is a planning method to site and size chargers of EVs in distribution grids accounting for grid constraints, multiple charger typologies, and EV owners' flexibility in plugging and unplugging their EVs. The problem is formulated as an economic optimization and is based on a mixed-integer linear program (MILP) that can be solved with off-the-shelf optimization libraries. Results are developed for EVs with two different battery sizes to illustrate how this impacts recharging patterns and the final planning results.

The paper is organized as follows. Section II describes the problem statement, input quantities, and model assumptions. Section III describes the models adopted in the planning problem and its formulation. Section IV describes the model of EV owners' flexibility. Section V describes the synthetic case study adopted to test the models. Section VI presents results and discussions. Finally, Section VII concludes the paper.

## II. Preliminaries

### A. Problem statement

It is considered the perspective of an integrated grid operator/urban planner wishing to attain minimum capital investments to roll out the EV charging infrastructure in a power distribution grid. More specifically, the objective of the problem is to identify the location, rating (i.e., fast and slow charging), and the number of chargers in the grid to satisfy the charging demand of a given population of EVs at the minimum capital cost and while respecting the distribution grid's constraints.

Both single- and multi-port chargers are considered in the problem. This is to evaluate the techno-economical benefits of one or the other configuration, or a mixed one. The distinction between these two charger typologies is that SPCs have a plug for each charging column, whereas MPCs have a centralized AC/DC power conversion stage and multiple ports (each with a DC/DC converter to enable power flow control to each EV) to enable the connection of multiple EVs (Fig. 1). As an MPC might have a smaller AC/DC converter than a group of SPCs for the same number of plugs, it could lead to reducing capital investments for the charging infrastructure. From an operational perspective, MPCs enable arbitraging the charge among multiple vehicles, offering increased flexibility for congestion management. Because MPCs do not require the EV owners to plug and unplug their vehicles from and into a charger manually, they can also lead to optimized utilization of the chargers.

Although the proposed methodology is general and can be adapted to model arbitrary power rating of the charging stations, we specifically consider two charger ratings for SPCs, i.e., fast and slow chargers, with kVA rating denoted by $\bar{F}$ and $\bar{S}$ (with $\bar{F} > \bar{S}$), respectively. For MPCs, the charger rating is assumed to be a multiple of $\bar{S}$ or $\bar{F}$.
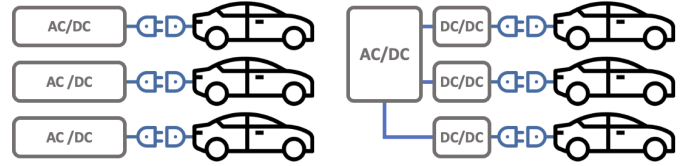


Fig. 1: Single-port chargers (SPCs) on the left, and multi-port chargers (MPCs) on the right.

### B. Input information and notation

This section introduces the notation and input information used in the problem. Let index $n = 1, \ldots, N$ denote the nodes of the power grid (see for example Fig. 5), $t = 1, \ldots, T$ the time intervals, and $v = 1, \ldots, V$ the EVs. $N$, $T$, and $V$ are the total numbers of nodes, intervals and vehicles, respectively.

*1) Input information for EVs:* The inputs are the parking location over time, the EV battery discharging power due to driving, and the energy storage capacity of the EV batteries.

The EVs' parking locations are encoded in the following input binary parameters:

$$p_{nvt} = \begin{cases} 1, & \text{if EV } v \text{ is connected to node } n \text{ at time } t \\ 0, & \text{otherwise.} \end{cases} \quad (1)$$

The subscript "$nvt$", and similarly other subscripts introduced in the paper, denotes quantities for node $n$ and vehicle $v$ at time interval $t$, and not the product among these indexes. It is illustrative to mention that because a vehicle can be parked at one node only, the following inequality holds:

$$\sum_{n=1}^{N} p_{nvt} \le 1 \qquad \forall t \text{ and } v. \quad (2)$$

The EV battery discharging power is denoted by $p_{vt}^{\text{EV-}}$. This quantity depends primarily on the driving/transportation demand, but also on other factors, such as driving style and regenerative breaking, auxiliaries' consumption (e.g., [20]), battery self-discharge, and battery state in general. Because this discharging power is an input quantity, the method proposed in this paper is independent from the specific way it is computed. For example, it can be computed by way of transport simulations (e.g., [21]), or estimated from experimental measurements or statistics (e.g., [22]–[24]).

Finally, the energy storage capacity of the EVs is denoted by $E_v$.

All these inputs will be exemplified in the case study description in Section V.

*2) Input information for the power grid:* The inputs are the grid topology, lines characteristics, and nodal injections due to demand and distributed generation. These pieces of information are necessary to model the operational constraints of the distribution grid with (linearized) load flow equations so as to produce chargers deployment plans that are respectful of grid constraints. They will be formalized when introducing the grid model.

### C. Overview of the modeling principles and optimization problem

Figure 2 depicts and introduces all the modeling elements involved in the planning problem. The figure is now explained, from top to bottom. At the top of the figure (black and dark yellow boxes), the evolution in time of the vehicles' SOCs is computed as a function of the battery discharging power due to driving. In order to keep the EVs in a functional state and satisfy the driving demand of the EV owners, the SOCs should be within the physical limits (e.g., between 10% and 100%, or any other configurable range). To this end, the problem computes when recharging the EVs (red box): a prerequisite for an EV to be charged is being plugged into a charger (first blue box from the top), which is in turn possible only when a vehicle is parked (this information is available from the input variables $p_{nvt}$, discussed in the former section). The EV plugged-in state does not depend on its parking state only but also on i) a charger availability and ii) EV owners' availability to unplug a charged EV and plug in an EV that needs to be recharged. For example, it is unlikely that an EV is plugged into a charger in the early morning hours as its owner might sleep: this flexibility of the owner is specifically modeled with a dedicated set of constraints, as explained in Section IV.

An additional constraint of the charging problem is that charging an EV should not engender violations of the grid operational constraints (green box); the parking location of the EVs (known from $p_{nvt}$) establishes the link between the EVs' recharging demand and the power demand at the grid's nodes, allowing to model grid quantities.

Once all the charging schedules are determined (grey boxes), they are used to evaluate how many chargers are needed to meet the recharging demand. The total number of chargers is finally used to assess the total cost of the infrastructure, which is the objective function that the problem minimizes. An additional set of constraints (denoted by the last blue box) models whether SPCs or MPCs are allowed in the problem.

The problem is an economical cost minimization formulated as a MILP program. The problem formulation is presented in sections III and IV. In particular, elements are introduced in the following order:

- section III-A describes the EVs recharging model;
- III-B explains the models of the SPCs, MPCs, and the cost function of the planning problem.
- III-C formulates the grid nodal injections based on the EVs' recharging demand and the power grid's constraints;
- III-D presents the complete formulation of the optimization problem;
- III-E describes a linear approximation of the nonlinear optimization problem;
- III-F extends the model to V2G;
- finally, Section IV describes the constraints to model the EV owners' plugging-in and unplugging behaviors.

It is worth remarking that a byproduct of the planning problem illustrated in Fig. 2 is the optimal recharging policy that EV owners should adopt to recharge their vehicles. In this respect, the proposed model assumes that EV owners follow
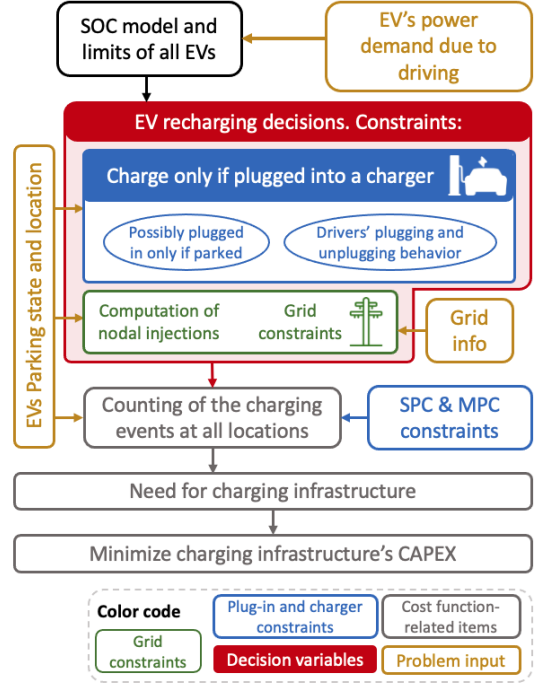


Fig. 2: The main elements used in the planning problem.

these recharging policies and that the operator can reliably estimate their recharging needs.

## III. METHODS

The problem is formulated as a constrained economic optimization program with the objective of minimizing the capital investment of the chargers subject to meeting the EVs' recharging demand and respecting the grid's operational requirements. All these elements are described here below.

### A. Plugged-in state, charging power, and SOC of the electric vehicles

*1) Modeling connection and charging state:* For each vehicle $v$ and time interval $t$, the binary variables $f_{vt}^{\mathrm{plugged}}, s_{vt}^{\mathrm{plugged}}$ define whether the EV is plugged into a fast and a slow charger, respectively. As an EV cannot be connected to a fast and slow charger simultaneously, it holds that $f_{vt}^{\mathrm{plugged}}$ and $s_{vt}^{\mathrm{plugged}}$ cannot be active at the same time; moreover, as an EV can be plugged only when parked, $f_{vt}^{\mathrm{plugged}}$ and $s_{vt}^{\mathrm{plugged}}$ can be active only if at least one $p_{nvt}$ among all nodes is active. These two requirements can be formalized in the following inequality constraint:

$$f_{vt}^{\mathrm{plugged}} + s_{vt}^{\mathrm{plugged}} \leq \sum_{n=1}^{N} p_{nvt} \qquad \forall t \text{ and } v. \qquad (3)$$

Two additional binary variables per vehicle and time interval, denoted by $f_{vt}^{\mathrm{charge}}, s_{vt}^{\mathrm{charge}}$, indicate whether a vehicle $v$ is charging from a fast or a slow charger at time $t$. As EVs can charge only when plugged into a charger, it holds that:

$$f_{vt}^{\mathrm{charge}} \leq f_{vt}^{\mathrm{plugged}} \qquad \forall t \text{ and } v \qquad (4a)$$

$$s_{vt}^{\mathrm{charge}} \leq s_{vt}^{\mathrm{plugged}} \qquad \forall t \text{ and } v \qquad (4b)$$

Quantities $f_{vt}^{\text{plugged}}$, $s_{vt}^{\text{plugged}}$, $f_{vt}^{\text{charge}}$, $s_{vt}^{\text{charge}}$ are variables of the optimization problem; based on these variables, the charging power of the EVs, as well as the needs for fast and slow chargers are determined, as it will be explained next.

*2) Charging power:* With the above definitions in place, the charging power of a vehicle $v$ and time $t$ is:

$$p_{vt}^{\text{EV+}} = f_{vt}^{\text{charge}} \cdot \bar{F} \cdot \cos\phi_F + s_{vt}^{\text{charge}} \cdot \bar{S} \cdot \cos\phi_S, \quad (5a)$$

where input parameters $\bar{F}$ and $\cos\phi_F$ are the kVA rating and power factor of the fast charger, respectively, and similarly for $\bar{S}$ and $\cos\phi_S$. The reactive power associated to this charging demand is:

$$q_{vt}^{\text{EV+}} = f_{vt}^{\text{charge}} \cdot \bar{F} \cdot \sin\phi_F + s_{vt}^{\text{charge}} \cdot \bar{S} \cdot \sin\phi_S. \quad (5b)$$

It is worth highlighting that chargers are assumed to be operated on and off, in other words the recharging power cannot be modulated in intensity. However, the recharging power of all chargers can be modulated in time, ultimately achieving power intensity modulation at the aggregated level and allowing for grid congestion management.

*3) Vehicles' state-of-charge (SOC):* The evolution of the vehicles' SOC depends on the charging power $p_{vt}^{\text{EV+}}$, given by (5a), and the discharging power $p_{vt}^{\text{EV-}}$, which is an input of the problem. The SOC of vehicle $v$ at time $t$ is modeled as:

$$\text{SOC}_v(t) = \text{SOC}_v(0) + \frac{T_s}{E_v} \sum_{\tau=0}^{t-1} \left( \eta \cdot p_{v\tau}^{\text{EV+}} - p_{v\tau}^{\text{EV-}} \right), \quad (6)$$

where $\text{SOC}_v(0)$ is the initial SOC (a problem decision variable, as it will be discussed later), $T_s$ the sampling time in hours, $E_v$ the nominal energy capacity of the EV's battery (in kWh), and $\eta$ is the charging efficiency.

It is worth highlighting that since the discharging power is assumed estimated directly from the vehicles' SOCs, it is not weighted by the efficiency in (6).

Model (6) is linear in the charging power. This model, commonly adopted in the literature (e.g. [25]), assumes constant battery's voltage and efficiency. These assumptions, which trade-off accuracy for increased model tractability, can be considered acceptable in a planning problem with sparse temporal resolution (e.g., 1 hour). The vehicles' SOCs should be within a feasible range, denoted by $(\underline{\text{SOC}}, \overline{\text{SOC}})$. This constraint reads as:

$$\underline{\text{SOC}} \leq \text{SOC}_v(t) \leq \overline{\text{SOC}}. \quad (7)$$

### B. Identifying the need for charging infrastructure

It is now explained how the number of chargers and their locations are identified. Based on the number of chargers, the capital investment of the charging infrastructure is then modeled.

*1) Single-port chargers:* It is first considered the case of single-port chargers, which feature an equal number of plugs and chargers (Fig. 1). The following explanation refers to fast chargers; for slow chargers, the principles are identical and not repeated.

The modeling principle used to compute the number of chargers to install consists in evaluating the maximum number of chargers in use at each grid node. For example, if at node 2, a maximum of 10 vehicles are simultaneously plugged into a charger over the whole planning horizon, then 10 chargers will be necessary to meet the demand for chargers at this node. This modeling principle is now formalized.

The number of fast chargers in use at a specific grid node can be evaluated by coupling the information in $f_{vt}^{\text{plugged}}$ (telling whether an EV is plugged into a charger) and $p_{nvt}$ (the EV parking location). More specifically, the number of fast chargers in use at time interval $t$ at node $n$ is the sum over all vehicles of the product between $p_{nvt}$ and $f_{vt}^{\text{plugged}}$. The maximum value over time of this expression is the required number of fast chargers to be installed, denoted by $F_n^{\text{chargers}}$. Formally, it is:

$$F_n^{\text{chargers}} = \max_t \left\{ \sum_{v=1}^{V} p_{nvt} \cdot f_{vt}^{\text{plugged}} \right\}, \quad n = 1, \dots, N. \quad (8a)$$

Because SPC chargers have one plug per charger by design, the number of available plugs must match the number of chargers. Say $F_n^{\text{plugs}}$ is the number of plugs, then the following equality constraint must hold:

$$F_n^{\text{plugs}} = F_n^{\text{chargers}}. \quad (8b)$$

For slow chargers, similar expressions hold:

$$S_n^{\text{chargers}} = \max_t \left\{ \sum_{v=1}^{V} p_{nvt} \cdot s_{vt}^{\text{plugged}} \right\}, \quad n = 1, \dots, N \quad (8c)$$

$$S_n^{\text{plugs}} = S_n^{\text{chargers}}. \quad (8d)$$

where $S_n^{\text{chargers}}$ and $S_n^{\text{plugs}}$ are the number of chargers and of plugs, respectively.

*2) Multi-port chargers:* Differently than a SPC, a single MPC can have have multiple plugs. The numbers of plugs and chargers now follow from different models, as explained hereafter.

The number of fast chargers is calculated considering the variables $f_{vt}^{\text{charge}}$, which tell, for a given time $t$, how many vehicles are recharging at the same time, so providing information on the rated power required to meet the realized recharging demand. Following the same principle discussed above for SPCs, coupling this information with $p_{nvt}$ enables to locate this power demand in the grid. Formally, the number of fast and slow MPCs is:

$$F_n^{\text{chargers}} = \max_t \left\{ \sum_{v=1}^{V} p_{nvt} \cdot f_{vt}^{\text{charge}} \right\}, \quad n = 1, \dots, N \quad (9a)$$

$$S_n^{\text{chargers}} = \max_t \left\{ \sum_{v=1}^{V} p_{nvt} \cdot s_{vt}^{\text{charge}} \right\}, \quad n = 1, \dots, N. \quad (9b)$$

The number of plugs for, e.g., fast chargers is instead calculated considering the variables $f_{vt}^{\text{plugged}}$, which provide the information of how many vehicles are connected to a charger

at the same time. Formally, the numbers of plugs for fast and slow chargers are:

$$F_n^{\text{plugs}} = \max_t \left\{ \sum_{v=1}^{V} p_{nvt} \cdot f_{vt}^{\text{plugged}} \right\}, \quad n = 1, \ldots, N \quad (9c)$$

$$S_n^{\text{plugs}} = \max_t \left\{ \sum_{v=1}^{V} p_{nvt} \cdot s_{vt}^{\text{plugged}} \right\}, \quad n = 1, \ldots, N. \quad (9d)$$

It is worth to highlight that the planning problem for MPCs is a generalization of the one of SPCs. This is because, if the solution of the MPCs' problem is such that $f_{vt}^{\text{charge}} = f_{vt}^{\text{plugged}}$ and $s_{vt}^{\text{charge}} = s_{vt}^{\text{plugged}}$ for all $v$ and $t$, then formulations in (9) and (8) are the same and the two problems would have the same solution.

*3) Investment costs for the charging infrastructures:* Based on the required numbers of plugs and chargers, we can estimate the capital cost of the charging infrastructure. The total investment cost is denoted by $J(\cdot)$, where notation $(\cdot)$ refers to the dependency of $J$ on the problem decision variables $f_{vt}^{\text{plugged}}$, $s_{vt}^{\text{plugged}}$, $f_{vt}^{\text{charge}}$, and $s_{vt}^{\text{charge}}$, which is not explicitly reported for compactness. It reads as:

$$J(\cdot) = J_{plugs}^F + J_{chargers}^F + J_{plugs}^S + J_{chargers}^S \quad (10a)$$

where $J_{plugs}^F$, $J_{chargers}^F$ are the cost of fast-charging plugs and stations, and $J_{plugs}^S$ and $J_{chargers}^S$ are the cost of slow-charging plugs and stations. The components of (10a) are as follows:

$$J_{plugs}^F = \sum_{n=1}^{N} F_n^{\text{plugs}} \cdot \text{cost}_{plugs}^F \quad (10b)$$

$$J_{plugs}^S = \sum_{n=1}^{N} S_n^{\text{plugs}} \cdot \text{cost}_{plugs}^S \quad (10c)$$

$$J_{chargers}^F = \sum_{n=1}^{N} F_n^{\text{chargers}} \cdot \text{cost}_{chargers}^F \quad (10d)$$

$$J_{chargers}^S = \sum_{n=1}^{N} S_n^{\text{chargers}} \cdot \text{cost}_{chargers}^S \quad (10e)$$

where $\text{cost}_{plugs}^F, \text{cost}_{chargers}^F, \text{cost}_{plugs}^S, \text{cost}_{chargers}^S$ are the unitary cost of plugs and chargers for fast and slow charging. Service life and maintenance of all these components are assumed the same regardless of their use and cycle ageing (e.g., [26]), so their unitary costs can be directly compared in the cost function without rescaling them.

*C. Nodal injections due to EVs charging demand and grid model*

The problem formulation so far has focused on modeling the connection of EVs to chargers, the EVs' charging process, and how these reflect on the cost of the charging infrastructure. In this section, the charging demand of the EVs is used in a grid's load flow model to assess whether grid constraints are respected. These additional constraints are implemented in the planning problem with the specific objective of locating the chargers in the distribution grid without engendering violations

of its operational limits. As load flow models are nonconvex, we resort to a linearized load flow based on sensitivity coefficients, as proposed in [27]–[30], to retain the problem's tractability.

We denote the total charging demand for the EVs connected to node $n$ by $P_{nt}^{\text{EV}}$, and the associated reactive power demand by $Q_{nt}^{\text{EV}}$. These quantities are computed by coupling the information on the charging power of the individual EVs, $p_{vt}^{\text{EV+}}$ in (5), with their parking location, $p_{nvt}$. Formally, they are:

$$P_{nt}^{\text{EV}} = \sum_{v=1}^{V} p_{nvt} \cdot p_{vt}^{\text{EV+}} \qquad \forall t \text{ and } n \quad (11a)$$

$$Q_{nt}^{\text{EV}} = \sum_{v=1}^{V} p_{nvt} \cdot q_{vt}^{\text{EV+}} \qquad \forall t \text{ and } n. \quad (11b)$$

The nodal power injections at the various nodes of the distribution grid are given by the total charging demand of the EVs in (11) along with conventional demand and local distributed generation. Conventional demand and distributed generation is modeled in terms of net demand, denoted by $P_{nt}^{\text{net}}$, given by the difference between the two. The net demand is an input of the problem. Nodal active and reactive power injections read as:

$$P_{nt}^{\text{node}} = \sum_{v \in \mathcal{V}} p_{nvt} \cdot p_{vt}^{\text{EV+}} + P_{nt}^{\text{net}} \quad (12a)$$

$$Q_{nt}^{\text{node}} = \sum_{v \in \mathcal{V}} p_{nvt} \cdot q_{vt}^{\text{EV+}} + Q_{nt}^{\text{net}}. \quad (12b)$$

Because the grid voltage is constrained in a narrow band, we use the approximation that nodal power injections are voltage-independent. Voltage-dependent power injections, that could be integrated into the linearized grid model as proposed in [31], will be considered in future works.

Nodal voltage magnitudes $v_{tn}$, line current magnitudes $i_{tl}$ in lines $l = 1, \ldots, L$, and apparent power flow at the substation transformer $S_{t0}$ are denoted with the following notation

$$v_{tn} = f_n \left( P_{t1}^{\text{node}}, \ldots, P_{tN}^{\text{node}}, Q_{t1}^{\text{node}}, \ldots, Q_{tN}^{\text{node}} \right) \quad (13a)$$

$$i_{tl} = g_l \left( P_{t1}^{\text{node}}, \ldots, P_{tN}^{\text{node}}, Q_{t1}^{\text{node}}, \ldots, Q_{tN}^{\text{node}} \right) \quad (13b)$$

$$S_{t0} = h_l \left( P_{t1}^{\text{node}}, \ldots, P_{tN}^{\text{node}}, Q_{t1}^{\text{node}}, \ldots, Q_{tN}^{\text{node}} \right) \quad (13c)$$

which highlights the dependency between grid quantities and nodal injections through the functions $f_n$, $g_l$, and $h_l$. The problem dependency on the admittance matrix (i.e., topology and cables' characteristics), and slack bus voltage are omitted from this notation for simplicity. Using the notion of sensitivity coefficients, functions $f_n$, $g_l$, and $h_l$ can be expressed as a linear function of the nodal power injections around linearization points (assumed given).

Operational constraints of the distribution grid are nodal voltage magnitudes within prescribed limits $(\underline{v}, \overline{v})$, currents in the lines below the lines' ampacities $\overline{i}_l$, and power flow at the substation transformer less than its rating $\overline{S}_0$. These reads as:

$$\underline{v} \leq v_{tn} \leq \overline{v} \qquad \forall t \text{ and } n \quad (13d)$$

$$|i_{tl}| \leq \overline{i}_l \qquad \forall t \text{ and } l \quad (13e)$$

$$S_{t0} \leq \overline{S}_0 \qquad \forall t. \quad (13f)$$

In addition to these constraints, we require nodal injections to be below the apparent power limit of the node, $S_n$:

$$(P_{nt}^{\text{node}})^2 + (Q_{nt}^{\text{node}})^2 \leq (S_n)^2. \tag{13g}$$

Constraint (13g) is useful in the case of apparatus with apparent power limitations connected at the nodes, such as nodes hosting substation step-down transformers.

### D. Planning problem

The planning problem consists in finding the binary variables

$$\boldsymbol{x} = [f_{11}^{\text{charge}}, \ldots, f_{VT}^{\text{charge}}, s_{11}^{\text{charge}}, \ldots, s_{VT}^{\text{charge}}] \tag{14}$$

$$\boldsymbol{y} = [f_{11}^{\text{plugged}}, \ldots, f_{VT}^{\text{plugged}}, s_{11}^{\text{plugged}}, \ldots, s_{VT}^{\text{plugged}}] \tag{15}$$

that minimize the capital investment for the EV charging infrastructure while subject to grid constraints.

To avoid that the problem solution depend on the initial SOC values in (6), we choose to set them as problem variables, denoted by:

$$\boldsymbol{z} = [\text{SOC}_1(0), \ldots, \text{SOC}_V(0)] \in \mathbb{R}^V. \tag{16}$$

Besides, the final SOC should be larger than or equal to the initial one to avoid benefiting from the initial energy stock:

$$\text{SOC}_v(T) \geq \text{SOC}_v(0), \qquad \text{for all } v. \tag{17}$$

In this way, the planning problem accounts for the charging demand of the vehicles, regardless of their specific initial conditions.

The planning problem is formulated as a constrained economic optimization. Its formulation reads as:

$$\min_{\boldsymbol{x},\boldsymbol{y}\in\{0,1\}^{V\times T}, \boldsymbol{z}\in\mathbb{R}^V} \{J(\cdot)\} \tag{18a}$$

subject to the following constraints:

| | | |
|---|---|---|
| Plugged-in only if parked (3) | $\forall t$ and $v$ | (18b) |
| Charge only if plugged-in (4) | $\forall t$ and $v$ | (18c) |
| EV charging power (5) | $\forall t$ and $v$ | (18d) |
| SOC model and constraints (6), (7), (17) | $\forall t$ and $v$ | (18e) |
| Nodal injections (11) and (12) | $\forall t$ and $n$ | (18f) |
| Linear grid models and constraints (13) | | (18g) |
| Chargers and plugs number model: | | |
| (8) for SPCs, or (9) for MPCs | | (18h) |

### E. Problem properties and approximations

Problem (18) is nonlinear due to the set maximum in (8)-(9), the point-wise maximum in (25d) (a new constraint, explained in the next section), and the quadratic expression in (13g). Suitable reformulations or approximations of these constraints are now discussed to render the problem linear. The set maximum, here denoted by $\bar{v} = \max\{v_t, t = 1, \ldots, T\}$ for convenience, is replaced by $T$ linear inequalities $\bar{v} \geq v_t$ for all $t$. As the problem (18) entails *minimizing* expressions of the

same kind as $\bar{v}$, this reformulation holds as exact. The point-wise maximum, $a^+ = \max(a, 0)$, is replaced by 2 inequalities, $a^+ \geq a$ and $a^+ \geq 0$ and can be used to replace convex constraints in the form of $\max(a, 0) \leq \bar{a}$ with linear ones [32].

Finally, the apparent power constraint in (13g), now denoted by $P^2 + Q^2 \leq S^2$ for simplicity, is approximated by replacing the reactive power with an upper bound $\overline{Q} = S \cdot \overline{\sin}\phi$; since $Q \leq \overline{Q}$, it follows that:

$$P^2 + Q^2 \leq P^2 + \overline{Q}^2 \leq S^2 \tag{19a}$$

$$P^2 \leq S^2 - \overline{Q}^2 = S^2 - S^2 \cdot \overline{\sin}^2\phi = S^2 \underline{\cos}^2\phi \tag{19b}$$

$$P \geq -S \cdot \underline{\cos}\phi \quad \text{and} \quad P \leq S \cdot \underline{\cos}\phi. \tag{19c}$$

In summary, the original quadratic constraint is replaced by two linear inequalities, (19c), with $\underline{\cos}\phi$ as a lower-bound estimate of the load power factor. An alternative approach is to approximate the convex set (13g) with linear inequalities (e.g., [33]), typically preferrable when reactive power is an explicit control variable of the problem. With these equivalent formulations and approximation, it is possible to write the optimization problem as a mixed integer linear problem (MILP).

### F. Extension to V2G

It is shown here how the formulation can be extended to model V2G support from the EVs with bidirectional chargers. For brevity, this is shown for slow chargers only. For fast chargers, similar equations can be derived by replacing the relevant variables.

Similarly to the binary variable $s_{vt}^{\text{charge}}$ that denotes if an EV is recharging or not, we introduce a new binary variable, $s_{vt}^{\text{discharge}}$, that indicates whether an EV is discharging. Because an EV can either be charged or discharged at the same time, and can be discharged only when plugged, the following two constraints must hold:

$$s_{vt}^{\text{discharge}} + s_{vt}^{\text{charge}} \leq 1, \tag{20}$$

$$s_{vt}^{\text{discharge}} \leq s_{vt}^{\text{plugged}}, \qquad \forall t \text{ and } v. \tag{21}$$

The V2G power is:

$$p_{vt}^{\text{V2G}} = s_{vt}^{\text{discharge}} \cdot \bar{S} \cdot \cos\phi_S. \tag{22}$$

The SOC model in (6) now needs to account for the discharging power too. The update model reads as:

$$\text{SOC}_v(t) = \text{SOC}_v(0) + $$
$$+ \frac{T_s}{E_v} \sum_{\tau=0}^{t-1} \left( \eta p_{v\tau}^{\text{EV+}} - p_{v\tau}^{\text{EV-}} - \frac{1}{\eta} p_{vt}^{\text{V2G}} \right) \quad \forall v \tag{23}$$

Finally, the nodal injections model are modified to include the contribution of V2G:

$$P_{nt}^{\text{node}} = \sum_{v\in\mathcal{V}} p_{nvt} \cdot \left( p_{vt}^{\text{EV+}} - p_{vt}^{\text{V2G}} \right) + P_{nt}^{\text{net}}. \tag{24}$$

## IV. Modeling EV connection and disconnection preferences

It has been said that $f_{vt}^{\text{plugged}}$ and $s_{vt}^{\text{plugged}}$ (denoting if an EV is plugged into a charger) can be active only when an EV is parked. However, there is more. Because plugging an EV into a charging column is an operation performed by the EV owner (or driver), their availability to plug and unplug an EV should also be modeled. For example, a person driving home in the evening and using a public charging column might prefer to plug their EV at the arrival rather than queuing for a charger to become available. To model this preference, we introduce additional constraints on $f_{vt}^{\text{plugged}}$ and $s_{vt}^{\text{plugged}}$ to capture two scenarios of EV owners' flexibility for plugging and unplugging their EVs. To explain these constraints, we refer to the case study analyzed in this paper, which is a home-work commute where EVs are used in the morning, parked in the central part of the day, used again in the afternoon, and finally parked overnight (as encoded in the input parameters $p_{nvt}$). The constraints to model EV owners' flexibility are discussed in the rest of this section.

### A. Modeling connection to and disconnection from chargers

Before describing the EV owners' flexibility scenarios, the models of connection-to-a-charger and disconnection-from-a-charger events are explained. For fast chargers, let binary variables $c_{vt}^f, d_{vt}^f$ denote the events when EV $v$ is connected to and disconnected from a charger, respectively, and similarly for slow chargers, with variables $c_{vt}^s$ and $d_{vt}^s$. In these variables, the logical state "1" denotes a connection or a disconnection event, and 0 no event. Connections and disconnections are modeled by detecting rising and falling edges of $f_{vt}^{\text{plugged}}$ and $s_{vt}^{\text{plugged}}$ (Fig. 3). Formally, this is as (with max as the point-wise maximum):

$$c_{vt}^f = \max\left(f_{vt}^{\text{plugged}} - f_{v(t-1)}^{\text{plugged}}, 0\right) \qquad \forall t \text{ and } v \quad (25a)$$

$$d_{vt}^f = \max\left(f_{v(t-1)}^{\text{plugged}} - f_{vt}^{\text{plugged}}, 0\right) \qquad \forall t \text{ and } v \quad (25b)$$
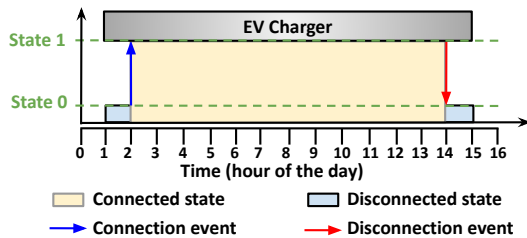
$$c_{vt}^s = \max\left(s_{vt}^{\text{plugged}} - s_{v(t-1)}^{\text{plugged}}, 0\right) \qquad \forall t \text{ and } v \quad (25c)$$

$$d_{vt}^s = \max\left(s_{v(t-1)}^{\text{plugged}} - s_{vt}^{\text{plugged}}, 0\right) \qquad \forall t \text{ and } v. \quad (25d)$$



Fig. 3: Example of the connection-state variable ($f_{vt}^{\text{plugged}}$ or $s_{vt}^{\text{plugged}}$) and connection and disconnection events (blue and red arrows), corresponding to the raising and falling edges of the connection state, respectively.

### B. EV owners' (drivers) flexibility scenarios

Let the time interval $(\tau_v^{(1)}, \tau_v^{(2)})$ denote the overnight parking stay, and $(\tau_v^{(3)}, \tau_v^{(4)})$ the parking stay during the central hours of the day for vehicle $v$. The two EV owners' flexibility scenarios are as follows.

**Scenario A (forgetful EV owners)**: *In both parking intervals, drivers plug their EVs to a charger only at the arrival time, and unplug them only at the departure time.* In other words, drivers let their vehicles plugged into a charger whenever their EVs is parked. Formally, this is implemented by enforcing no connection outside the initial parking time interval (for both fast and slow chargers)

$$c_{vt}^f \leq 0 \qquad \text{for all } t \text{ except } t = \tau_v^{(1)} \text{ and } t = \tau_v^{(3)} \quad (26a)$$

$$c_{vt}^s \leq 0 \qquad \text{for all } t \text{ except } t = \tau_v^{(1)} \text{ and } t = \tau_v^{(3)}, \quad (26b)$$

and no disconnection outside the final parking time interval

$$d_{vt}^f \leq 0 \qquad \text{for all } t \text{ except } t = \tau_v^{(2)} \text{ and } t = \tau_v^{(4)} \quad (26c)$$

$$d_{vt}^s \leq 0 \qquad \text{for all } t \text{ except } t = \tau_v^{(2)} \text{ and } t = \tau_v^{(4)}. \quad (26d)$$

**Scenario B (cooperative EV owners)**: *For overnight parking, drivers plug their EVs to a charger only at the arrival time, and unplug them only at the departure time; when parking in the central part of the day, drivers allow one disconnection.* In the central part of the day, drivers allow one disconnection to give to others the possibility of using that charging spot. This is implemented by enforcing no connection outside the initial parking time for the overnight time interval

$$c_{vt}^f \leq 0 \qquad \text{for all } t \text{ except } t = \tau_v^{(1)} \quad (27a)$$

$$c_{vt}^s \leq 0 \qquad \text{for all } t \text{ except } t = \tau_v^{(1)}, \quad (27b)$$

and up to one disconnection in the central parking hours

$$\sum_{t=\tau_3}^{\tau_4} d_{vt}^f \leq 1, \quad (27c)$$

$$\sum_{t=\tau_3}^{\tau_4} d_{vt}^s \leq 1. \quad (27d)$$

### C. Implementing the scenarios

Scenarios are implemented by adding either (26) or (27) to the optimization problem in (18). A comparative analysis of these 2 scenarios is performed in the results section to evaluate the impact of EV owners' flexibility on the problem solution.

## V. Case study

This section describes the case study adopted to exemplify the operations of the proposed planning method.

The case study is reasonably guessed to reproduce a real possible scenario. However, the contributions of this paper do not depend on this specific case study; in particular, input information can be tuned or changed as a function of the specific situation to model, on the basis of, for example, information from the distribution grid operator and urban planner.

## A. Number of EVs and driving demand

It is considered a home-work commute where EVs are used in the morning, parked in the central part of the day, used again in the afternoon, and parked overnight at the origin node. The different parking (and charging) locations correspond to different nodes of the grid. The residential nodes where EVs are parked overnight are indicated as the green nodes ("Cluster 1") in Fig. 1, whereas the destination nodes are the purple nodes ("Cluster 2"). In total, there are 1'000 EVs in this grid. This value is chosen based on the rating of this power grid, and it is in line with other studies (e.g., [30], [34]). The origin and destination nodes of the EVs are assigned randomly and uniformly to all nodes hosting EVs. The number of EVs parked during the night and central hours are shown in Fig. 4a and 4b, respectively. The EVs' morning departures and arrivals are sampled from uniform distributions with values between hours 5-8 and 8-11, respectively; evening departures and arrivals are sampled from uniform distributions with values between hours 14-18 and 17-21. Based on this information, variables $p_{nvt}$ are then built. As remarked earlier, this is an input of the problem, and other methods can be used, including using real data.

The total energy demand for driving is estimated using data from [22]. The discharging power $p_{vt}^{\text{EV-}}$, necessary to model the SOC evolution in (6), is a positive constant quantity when the vehicle drives, and zero when the EV is parked. The discharging power is such that its total energy demand amounts to the quantity estimated above.

To illustrate the impact on the planning results, two different values for the EV battery's energy capacity are considered: 16 kWh and 60 kWh, under the same driving demand. The EVs' charging efficiency, $\eta$, is 0.95.

The statistics of the daily recharging demand for driving (mean value plus/minus three times the standard deviation) are $8.2 \pm 1.9$ kWh and $17.1 \pm 4.0$ kWh, for the EVs with smaller and larger batteries, respectively.

## B. Planning horizon

The planning horizon refers to how many temporal samples are considered in the optimization problem (parameter $T$). Because the number of variables of the optimization problem increases linearly with $T$ and the complexity of the (NP-hard) MILP problem increases exponentially with the number of variables, it is necessary to limit the value of $T$ to retain problem's tractability. In this paper, $T$ is set to 24 samples (i.e., 1 day with samples each 1 hour) for the 16 kWh battery and to 120 (i.e., 5 days) for the 60 kWh battery under the assumption that this interval is either a worst-case scenario of the driving demand or a pattern regularly occurring throughout the service life of the charging infrastructure. Other methods to attain a tractable formulation of the optimization problem are scenario reduction or decomposition methods to decompose the temporal dimension of the problem and will be considered in future works. A similar scalability issue would be encountered when extending to distribution grids with a much larger number of nodes, as this would require increasing the number $V$ of EVs involved in the problem. This aspect will be investigated in future works.

The reason for the longer optimization horizon for the larger batteries is that EVs with larger energy capacity can make multiple trips on a single charge and might not require to charge each day, possibly staggering the charging process and contributing to avoiding grid overloading. The 1-day-long demand profiles are replicated five times to attain the input time series for the 5-day planning period.
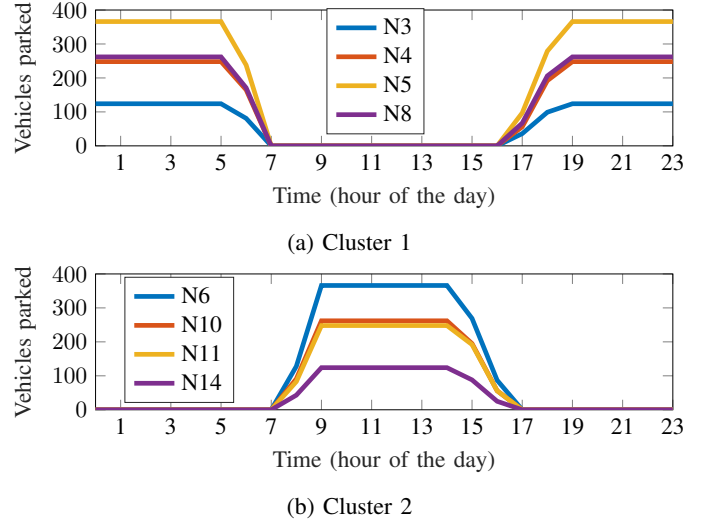


(a) Cluster 1



(b) Cluster 2

Fig. 4: Number of EVs' parked at different grid nodes under two clusters during the day and night hours.

## C. Chargers ratings and prices

We consider fast and slow chargers with kVA ratings of 20 kVA and 2.4 kVA, respectively, and power factors of 0.9. Their costs is 20'000€ and 1'500€, inspired from the existing technical literature [35]–[37] (although some price volatility might exist due to different regions, operators, and need for labor). The price of the charging plugs is assumed to be 15% of the price of a single-port charger.

## D. Distribution grid and demand

It is considered the European version of the 14-bus CIGRE benchmark grid for medium voltage (MV) systems [38] (Fig. 5). The low-voltage (LV) grids connected at the MV grid nodes are modeled in terms of their aggregated power. This modeling accounts for constraints of the rated power of the MV/LV substation transformer through (13g), and assumes that there are no violations of voltage levels and line ampacities in the LV grid. The MV grid is modeled as a single-phase equivalent assuming transposed conductors and loads balanced on the 3 phases. The demand of the grid is simulated considering the load profile proposed in [38], scaled according to the rated power of each node (Table I). At this stage, no distributed renewable generation is considered. The reactive power of the nodal injections is modeled assuming a constant power factor (Table I). Statutory voltage levels are $1 \pm 3\%$ per unit of the base voltage (20 kV). Line ampacities are according

to the conductor diameter. The sensitivity coefficients for the linearized grid model are computed once for the nominal demand profiles; one could compute successive linearizations to improve the linear estimates.

TABLE I: Nodal nominal demand and power factors

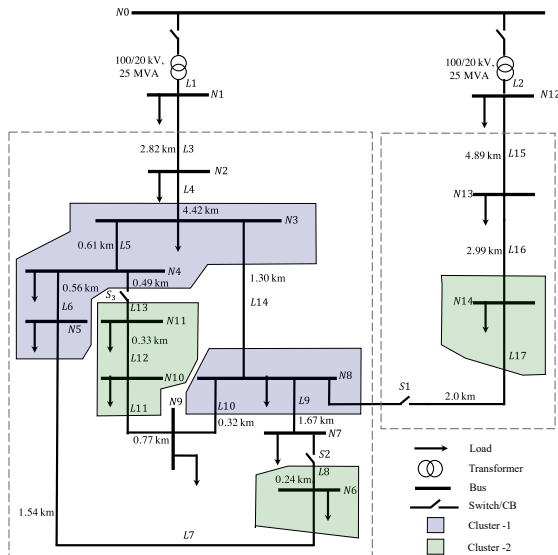| Node | Apparent Power [kVA] | Power factor | Cluster |
|---|---|---|---|
| 1 | 15'300 | 0.98 | - |
| 3 | 285 | 0.97 | 1 |
| 4 | 445 | 0.97 | 1 |
| 5 | 750 | 0.97 | 1 |
| 6 | 565 | 0.97 | 2 |
| 8 | 605 | 0.97 | 1 |
| 10 | 490 | 0.97 | 2 |
| 11 | 340 | 0.97 | 2 |
| 12 | 15'300 | 0.98 | - |
| 14 | 215 | 0.97 | 2 |



Fig. 5: Topology of the CIGRE European MV distribution network benchmark for residential system [38].

## VI. RESULTS AND DISCUSSIONS

We first present the results for the small-battery EVs to illustrate some of the formulation's properties. Then, the analysis is extended to the EVs with larger batteries. The accuracy of the linear grid estimates is discussed in Appendix A. The MILP problem is implemented in MATLAB and solved using Gurobi.

### A. Results for the 16 kWh EVs

This section presents the results for the EVs with small batteries and one-day-long optimization horizon. The optimization problem for 1'000 EVs is solved in about 90 minutes on an Intel i7 machine with a MIP gap setting of 10%.

Fig. 6 exemplifies the meaning of the variables $s_{vt}^{\mathrm{plugged}}$ and $s_{vt}^{\mathrm{charge}}$ for ten sample EVs in Scenario A and MPCs in order to illustrate their meaning. It shows that, i), vehicles are mostly connected to the chargers. This is in line with

the definition of Scenario A, which foresees EVs connected to the chargers whenever they are parked; ii), the planning algorithm arbitrages the charging of plugged EVs. This is done to respect grid constraints, ensure the EVs have correct SOC levels throughout the day and attain a minimum investment cost, as dictated by the problem cost function. We can thus infer that arbitraging the charge is beneficial to reducing the number of chargers, as explained hereafter.
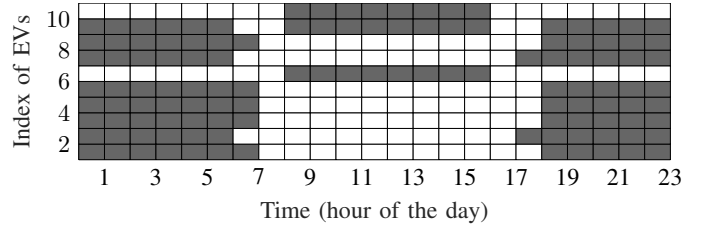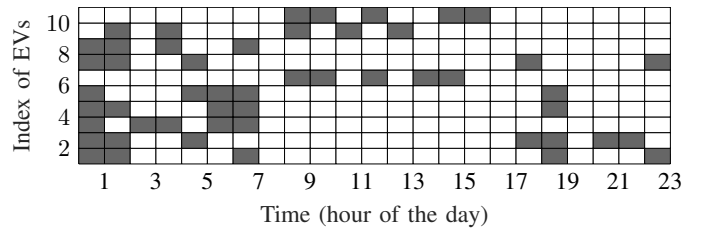


Fig. 6: Variables $s_{vt}^{\mathrm{plugged}}$ (a) and $s_{vt}^{\mathrm{charge}}$ (b), showing the connection and charging state, respectively, for 10 sample EVs. Grey filling is 1, white filling is 0.

The number of required chargers and plugs for SPCs, MPCs, and the two scenarios for driver's flexibility scenarios A and B are reported in Table II. For SPCs, the number of plugs is not indicated as it is the same as the number of chargers. The following findings can be derived.

**Finding 1**. Fast chargers are not required; (cheaper) slow chargers are enough to satisfy the charging demand.

**Finding 2**. Moving from forgetful (Scenario A) to cooperative EV owners (Scenario B) attains smaller numbers of chargers and plugs for both SPCs and MPCs. This is because increasing the availability of the EV owners to plug/unplug their EVs leads to better utilization of the charging infrastructure, ultimately requiring fewer chargers to satisfy the same charging demand.

**Finding 3**. Implementing MPCs requires less chargers (and more plugs) than SPCs; because the MPCs problem is a generalization of the SPCs' and the problem aims at finding the economic minimum, we can infer that MPCs are conducive to lower infrastructure costs. Fig. 7 summarizes the cost achieved by the various cases. MPCs achieve higher cost savings than cooperative EV owners: choosing MPCs over SPCs attains a cost reduction of 38% and 30% in Scenario A and B, respectively, whereas implementing cooperative EV owners (Scenario B) achieve a cost reduction of 13% and 3% for SPCs and MPCs, respectively. This has the interesting implication that a technological solution obtains a better effect than a change of consumer behavior.

**Finding 4**. Different scenarios and charger typologies (MPCs/SPCs) lead to a different spatial distribution of the chargers: chargers of Scenario A/SPCs are nearly equally split between the nodes of clusters 1 and 2, whereas Scenario B/SPCs has more chargers in Cluster 1, where vehicles are parked overnight. This is due to longer parking stays, which offer a higher potential for arbitrating the charge between a larger group of vehicles, leading to a more efficient use of the charging infrastructure.

TABLE II: Number of slow chargers and plugs (1'000 EVs, 16 kWh battery).

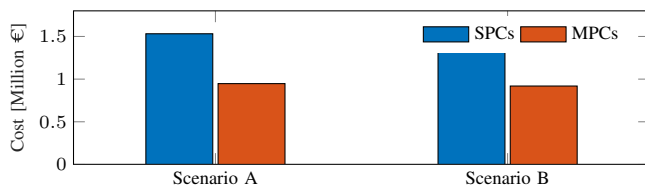| Node | Scenario A | | | Scenario B | | |
|---|---|---|---|---|---|---|
| | MPCs | | SPCs | MPCs | | SPCs |
| | Chargers | Plugs | Chargers | Chargers | Plugs | Chargers |
| 3 | 44 | 124 | 41 | 36 | 111 | 32 |
| 4 | 70 | 197 | 130 | 50 | 173 | 109 |
| 5 | 119 | 287 | 215 | 89 | 271 | 242 |
| 6 | 60 | 115 | 155 | 87 | 110 | 124 |
| 8 | 96 | 234 | 133 | 75 | 212 | 143 |
| 10 | 29 | 60 | 130 | 53 | 63 | 119 |
| 11 | 41 | 103 | 130 | 56 | 64 | 71 |
| 14 | 3 | 10 | 87 | 14 | 14 | 46 |
| Cluster1 | 329 | 842 | 519 | 250 | 767 | 526 |
| Cluster2 | 133 | 288 | 502 | 210 | 251 | 360 |
| Total | 462 | 1130 | 1021 | 460 | 1018 | 886 |



Fig. 7: Cost of the four cases.

Fig. 8 shows the distribution quantiles (in different shades of green) and median values (thick green line) of the injections of active power (conventional demand plus EVs) across the nodes over time. Nodal injections are scaled by the rated power of each node, so that one per unit (denoted by the horizontal dashed lines) corresponds to the maximum power flow at that node. Nodal injections and power transformer limits in (13g) were found to be the active constraints of the planning problem. In all the cases, the nodal injections hit the limit value in the evening hours. This is due to the combination of the evening's conventional demand and the EVs' charging demand. With SPCs, the grid is mostly loaded in the day's central hours, whereas with MPCs, the grid is mostly loaded in the afternoon and evening hours. This denotes that MPCs tend to shift the charging demand from the central part of the day to the afternoon and evening hours. This observation is in line with the previous consideration that the MPCs case has more chargers in the nodes corresponding to the overnight parking locations.

TABLE III: Number of slow chargers and plugs with V2G.

| Scenario A | | | Scenario B | | |
|---|---|---|---|---|---|
| MPCs | | SPCs | MPCs | | SPCs |
| Chargers | Plugs | Chargers | Chargers | Plugs | Chargers |
| 434 | 1005 | 1000 | 440 | 992 | 881 |

TABLE IV: Total EV charging demand versus V2G injections.

| | Scenario A | | Scenario B | |
|---|---|---|---|---|
| | SPCs | MPCs | SPCs | MPCs |
| Charging demand (kWh) | 15'062 | 10'893 | 10'768 | 10'338 |
| Discharging demand (kWh) | 1'246 | 257 | 553 | 112 |

Finally in this section, we evaluate whether V2G leads to lower development costs of the charging infrastructure. For a fair comparison with the former case, the cost of V2G chargers is assumed to be the same as the one-directional chargers. Table III shows the number of V2G chargers and plugs obtained by the planning problem. By comparing tables III and II, one can see that V2G achieves a slightly smaller number of total chargers, between 6% (Scenario A, MPCs) and 0.5% (Scenario B, SPCs). As the cost of the charging infrastructure is proportional to the number of chargers, the cost savings of V2G are also proportional. However, because the cost savings are comparable to the MIP gap setting adopted to solve the optimization problem (i.e., 10%), this gain is deemed as not specially significant. Table IV shows the total charging and discharging energy of the EVs, calculated as $\sum_{v,t} p_{vt}^{EV+}$ and $\sum_{v,t} p_{vt}^{V2G}$, respectively. The total discharging demand is a small fraction of the total charging demand, between 1% and 7%, denoting limited use of V2G. Overall, we can conclude that using V2G leads to marginal improvements in this case study.

### B. Results for the 60 kWh EVs

This section presents the results for the EVs with the larger battery size (60 kWh) and longer optimization horizon (5 days). The optimization problem is now solved with a MIP gap of 15% to reduce the computation time. In these settings, the optimization problem was solved in around 5 hours. Results are reported in Table V. We can derive the following observations.

**Finding 5**. Slow chargers are still the favourite choice of the planning problem.

**Finding 6**. The numbers of installed chargers/plugs are the same for MPCs and SPCs, as opposed to the former case with smaller batteries where there was a significant gap between these two numbers. This is because charging EVs takes longer when their battery is larger, assuming the same charging power and initial state-of-charge. Due to longer recharging times and the fact that chargers tend to be in operation whenever an EV is plugged in, the feature of swapping among several EVs (thanks to MPCs or increased driver flexibility) falls unused, without leading to more optimal use of the charging infrastructure. In support of this statement, we report the ratio between the EV's total charging time and the EV's total plugged in times for the SPC/Scenario A case, which is 0.60 for the smaller batteries and 0.83 for the larger ones, denoting longer recharging times and nearly saturated utilization factor of the charging infrastructure in the latter case.

**Finding 7**. The number of chargers (or plugs) required for the 60 kWh EVs is smaller than for the 16 kWh EVs. This is because EVs with smaller batteries need to be recharged more often, possibly at different nodes, thus requiring the
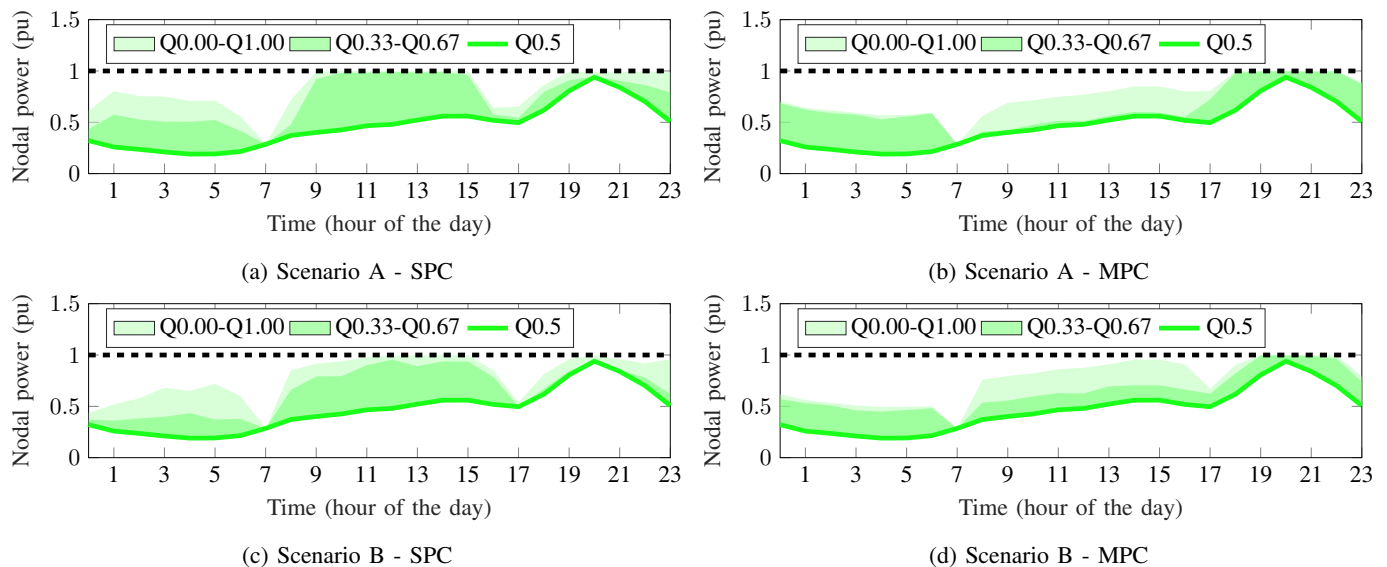
Fig. 8: Quantiles and median values of the active power injections across the grid nodes over time with the 16 kWh EVs.

installation of more chargers. Instead, EVs with larger batteries and more driving autonomy can perform multiple travels on a single charge and stagger the recharging process.

Finally, Fig. 9 shows the distribution quantiles of the nodal injections over the whole planning horizon. Compared to the case with smaller batteries which featured significant differences among the nodal injections for different chargers and EV owners' flexibility, nodal injections in the various cases are now similar.

TABLE V: Number of slow chargers and plugs (1'000 EVs, 60 kWh battery).

| Node | Scenario A | | | Scenario B | | |
|---|---|---|---|---|---|---|
| | MPCs | | SPCs | MPCs | | SPCs |
| | Chargers | Plugs | Chargers | Chargers | Plugs | Chargers |
| 3 | 62 | 59 | 59 | 62 | 63 | 64 |
| 4 | 140 | 142 | 140 | 139 | 140 | 142 |
| 5 | 235 | 237 | 236 | 236 | 237 | 236 |
| 6 | 127 | 130 | 127 | 127 | 127 | 127 |
| 8 | 146 | 146 | 153 | 149 | 149 | 153 |
| 10 | 78 | 78 | 80 | 78 | 78 | 78 |
| 11 | 76 | 77 | 76 | 76 | 76 | 77 |
| 14 | 31 | 28 | 32 | 28 | 28 | 27 |
| Cluster 1 | 583 | 584 | 588 | 586 | 589 | 595 |
| Cluster 2 | 312 | 313 | 315 | 309 | 309 | 309 |
| Total | 895 | 897 | 903 | 895 | 898 | 904 |

## VII. CONCLUSIONS

This paper presented a method to cost-optimally site and size chargers for EVs accounting for the constraints of the power distribution grid. The formulation considered both slow, fast, single-port, and multi-port chargers, and vehicle-to-grid. In addition, it included models to describe the flexibility of the EV owners (drivers) to plug and unplug their vehicles for optimized utilization of the charging infrastructure. By suitably modifying several nonconvex constraints appearing in the formulation, we derived a mixed-integer linear formulation of the problem that can be solved with off-the-shelf software libraries in a reasonable time. The method was applied on a

14-bus MV network considering a population of 1'000 EVs with two different EV battery sizes, 16 kWh and 60 kWh.

For the EVs with smaller batteries, results showed that multi-port chargers (MPCs) and cooperative EV owners are conducive to decreasing the number of chargers to install. However, with larger batteries, EV owners' flexibility and MPCs resulted in similar planning options as forgetful EV owners and SPCs. In the proposed case study, slow chargers were generally preferred over fast chargers. Simulation on a larger network with 30 nodes from [39] denoted similar findings.

The number of variables in the planning problem depends on the length of the optimization problem and on the number of vehicles. Because mixed-integer linear programs are NP-hard and their computation time drastically increases with the number of decision variables, carefully selecting the length of the input times series is needed to attain tractable computational times. In this work, this was done by selecting a short planning horizon (1 day for the smaller batteries, and 5 days for the larger one) under the assumption that inputs repeat periodically over the service life of the charging infrastructure. Similar conditions apply to the size of the network. Future work is in the direction of formulating problem approximations to increase the tractability of the problem when considering more extended input information.

## APPENDIX A
### ACCURACY OF THE LINEARIZED GRID MODELS

The accuracy of the linearized grid model is evaluated by comparing the linear estimates against the respective ground-truth quantities, which are computed by running a nonlinear load flow with the nodal injections from the optimization problem.

The histogram of the errors of the linear voltage and current estimations are shown in figures 11 and 12, respectively.

In the proposed case study, the active constraints of the problem were the nodal injections in (13g). It was verified

(a) Scenario A - SPC

(b) Scenario A - MPC

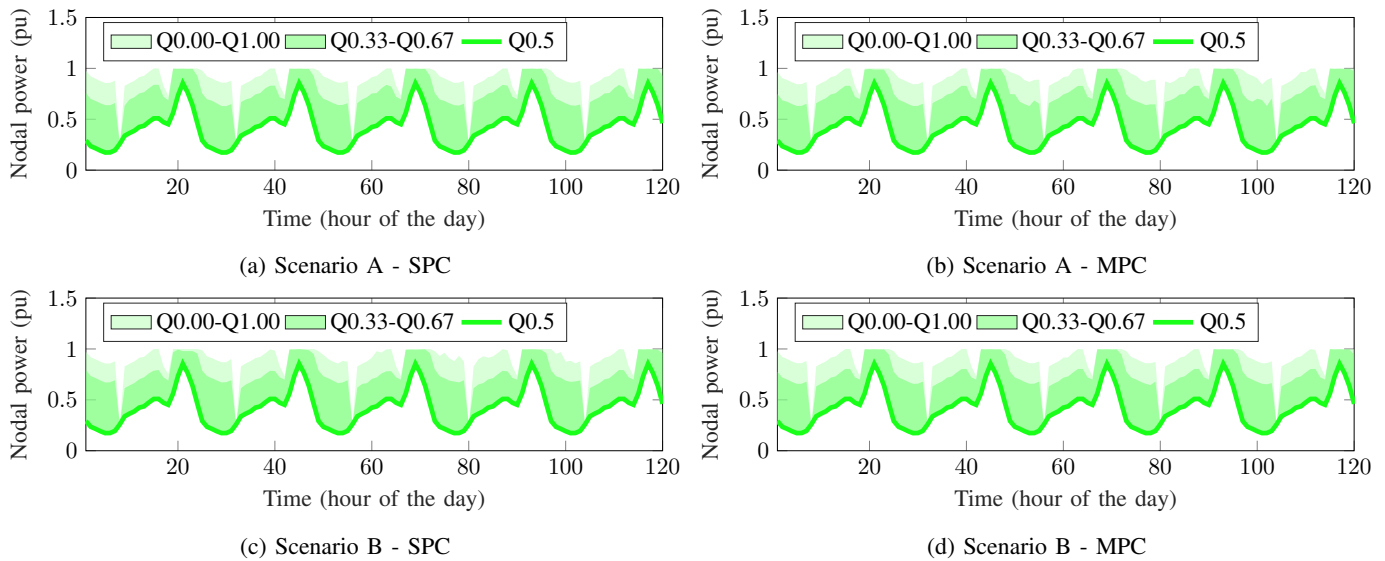(c) Scenario B - SPC

(d) Scenario B - MPC

Fig. 9: Quantiles and median values of the active power injections across the grid nodes over time with the 60 kWh EVs.
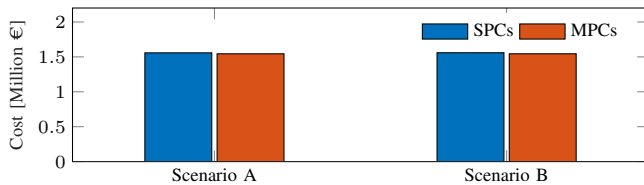


Fig. 10: Cost of the four cases for the extended 5-day long horizon.

that grid's voltage and current constraints would not have been violated even when accounting for the estimation errors of the linear model. However, in order to (conservatively) hedge against these modeling errors, one could add back-off terms to voltage and current constraints in (13d) and (13e) considering, for example, worst-case modelling errors from these histograms.

## REFERENCES

[1] "EU 2030 climate & energy framework," accessed: 2020-07. [Online]. Available: https://www.consilium.europa.eu/en/policies/climate-change/2030-climate-and-energy-framework/

[2] IRENA, "Innovation outlook: Smart charging for electric vehicles," International Renewable Energy Agency, Abu Dhabi, Tech. Rep. MSU-CSE-06-2, 2019.

[3] M.-O. Metais, O. Jouini, Y. Perez, J. Berrada, and E. Suomalainen, "Too much or not enough? Planning electric vehicle charging infrastructure: a review of modeling options." Feb. 2021, working paper or preprint. [Online]. Available: https://hal.archives-ouvertes.fr/hal-03127266

[4] "IEA, Electric car stock by region and technology, 2013-2018, IEA, Paris," https://www.iea.org/data-and-statistics/charts/electric-car-stock-by-region-and-technology-2013-2018, accessed: 2021-08.

[5] "Estimating electric vehicle charging infrastructure costs across major U.S. metropolitan areas," accessed: 2021-03. [Online]. Available: https://theicct.org/publications/charging-cost-US

[6] "Ministère de l'environnement de l'énergie et de lamer - La loi de transition Énergétique pour la croissance verte," accessed: 2021-03. [Online]. Available: https://bit.ly/3aRJ1Lb

[7] M. S. ElNozahy and M. M. A. Salama, "A comprehensive study of the impacts of PHEVs on residential distribution networks," *IEEE Transactions on Sustainable Energy*, vol. 5, no. 1, pp. 332–342, 2014.

[8] S. Johansson, J. Persson, S. Lazarou, and A. Theocharis, "Investigation of the impact of large-scale integration of electric vehicles for a swedish distribution network," *Energies*, vol. 12, 2019.

[9] H. Wang, Q. Huang, C. Zhang, and A. Xia, "A novel approach for the layout of electric vehicle charging station."

[10] Z. Hu and Y. Song, "Distribution network expansion planning with optimal siting and sizing of electric vehicle charging stations," in *2012 47th International Universities Power Engineering Conference (UPEC)*, 2012, pp. 1–6.

[11] Z. Liu, F. Wen, and G. Ledwich, "Optimal planning of electric-vehicle charging stations in distribution systems," *IEEE Transactions on Power Delivery*, vol. 28, no. 1, pp. 102–110, 2013.

[12] A. Y. S. Lam, Y.-W. Leung, and X. Chu, "Electric vehicle charging station placement: Formulation, complexity, and solutions," *IEEE Transactions on Smart Grid*, vol. 5, no. 6, pp. 2846–2856, 2014.

[13] C. Luo, Y.-F. Huang, and V. Gupta, "Placement of EV charging stations—balancing benefits among multiple entities," *IEEE Transactions on Smart Grid*, vol. 8, no. 2, pp. 759–768, 2017.

[14] H. Chen, Z. Hu, H. Luo, J. Qin, R. Rajagopal, and H. Zhang, "Design and planning of a multiple-charger multiple-port charging system for PEV charging station," *IEEE Transactions on Smart Grid*, vol. 10, no. 1, pp. 173–183, 2019.

[15] G. Liu, L. Kang, Z. Luan, J. Qiu, and F. Zheng, "Charging station and power network planning for integrated electric vehicles (EVs)," *Energies*, vol. 12, no. 13, 2019.

[16] Y. Xiang, J. Liu, R. Li, F. Li, C. Gu, and S. Tang, "Economic planning of electric vehicle charging stations considering traffic constraints and load profile templates," *Applied Energy*, vol. 178, pp. 647–659, 2016.

[17] J. Li, X. Sun, Q. Liu, W. Zheng, H. Liu, and J. A. Stankovic, "Planning electric vehicle charging stations based on user charging behavior," in *2018 IEEE/ACM Third International Conference on Internet-of-Things Design and Implementation (IoTDI)*, 2018, pp. 225–236.

[18] W. Gan, M. Shahidehpour, J. Guo, W. Yao, A. Paaso, L. Zhang, and J. Wen, "Two-stage planning of network-constrained hybrid energy supply stations for electric and natural gas vehicles," *IEEE Transactions on Smart Grid*, vol. 12, no. 3, pp. 2013–2026, 2021.

[19] W. Gan, M. Shahidehpour, M. Yan, J. Guo, W. Yao, A. Paaso, L. Zhang, and J. Wen, "Coordinated planning of transportation and electric power networks with the proliferation of electric vehicles," *IEEE Transactions on Smart Grid*, vol. 11, no. 5, pp. 4005–4016, 2020.

[20] L. De Vroey, R. Jahn, M. El Baghdadi, and J. Van Mierlo, "Plug-to-wheel energy balance-results of a two years experience behind the wheel of electric vehicles," *World Electric Vehicle Journal*, vol. 6, no. 1, pp. 130–134, 2013.

[21] K. W Axhausen, A. Horni, and K. Nagel, *The multi-agent transport simulation MATSim*. Ubiquity Press, 2016.
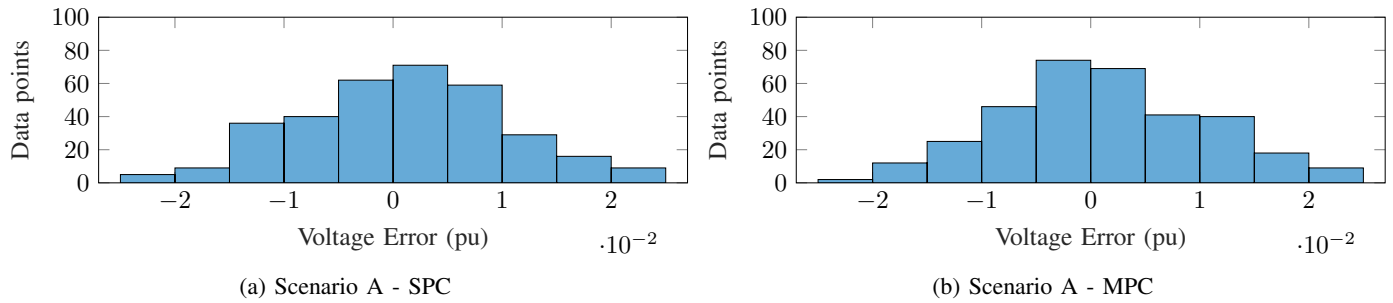
[22] "Test-an-EV project: Electrical vehicle (EV) data," http://mclabprojects.di.uniroma1.it/smarthgnew/Test-an-EV/?EV-code=EV8, accessed: 2020-02.

(a) Scenario A - SPC

(b) Scenario A - MPC

Fig. 11: Errors of the linear estimates of the nodal voltage magnitudes (in per unit of the base voltage).
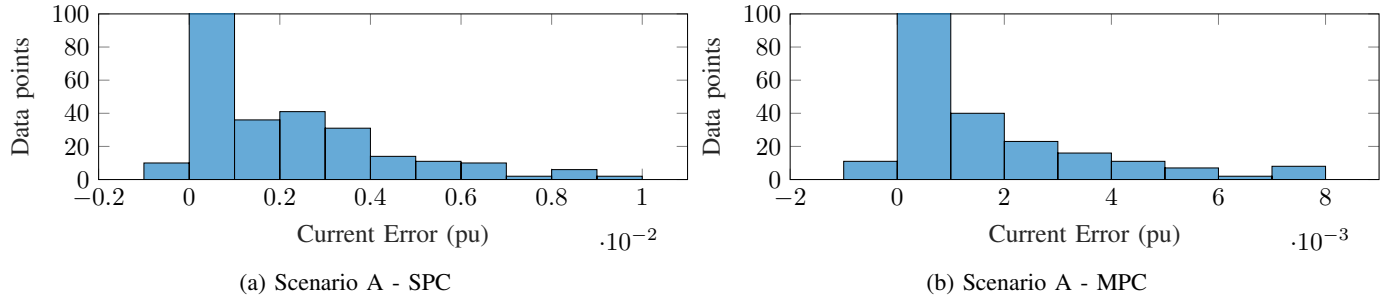


(a) Scenario A - SPC

(b) Scenario A - MPC

Fig. 12: Errors of the linear estimates of the lines' current magnitudes (per unit obtained by rescaling by the larger current observed in the grid).

[23] "Handbook of electric vehicle charging infrastructure implementation," NITY Aayog, Tech. Rep., August 2021.
[24] M. Gjelaj, S. Hashemi, P. B. Andersen, and C. Traeholt, "Optimal infrastructure planning for ev fast-charging stations based on prediction of user behaviour," *IET Electrical Systems in Transportation*, vol. 10, no. 1, pp. 1–12, 2020. [Online]. Available: https://ietresearch.onlinelibrary.wiley.com/doi/abs/10.1049/iet-est.2018.5080
[25] J. Van Roy, "Electric vehicle charging integration in buildings: Local charging coordination and dc grids," Ph.D. dissertation, KU Leuven, 2015.
[26] L. R. GopiReddy, L. M. Tolbert, and B. Ozpineci, "Power cycle testing of power switches: A literature survey," *IEEE Transactions on Power Electronics*, vol. 30, no. 5, pp. 2465–2473, 2014.
[27] K. Christakou, J. LeBoudec, M. Paolone, and D. Tomozei, "Efficient computation of sensitivity coefficients of node voltages and line currents in unbalanced radial electrical distribution networks," *IEEE Transactions on Smart Grid*, vol. 4, no. 2, pp. 741–750, 2013.
[28] F. Sossan, B. Mukherjee, and Z. Hu, "Impact of the charging demand of electric vehicles on distribution grids: a comparison between autonomous and non-autonomous driving," in *2020 Fifteenth International Conference on Ecological Vehicles and Renewable Energies (EVER)*, 2020, pp. 1–6.
[29] B. Mukherjee, G. Kariniotakis, and F. Sossan, "Smart charging, vehicle-to-grid, and reactive power support from electric vehicles in distribution grids: A performance comparison," in *2021 IEEE PES ISGT Finland (ISGT Europe)*, 2021.
[30] B. Mukherjee, G. Kariniotakis, and F. Sossan, "Scheduling the charge of electric vehicles including reactive power support: Application to a medium voltage grid," in *CIRED*, 2021.
[31] S. Fahmy and M. Paolone, "Analytical computation of power grids' sensitivity coefficients with voltage-dependent injections," in *2021 IEEE Madrid PowerTech*, 2021, pp. 1–6.
[32] S. Boyd, S. P. Boyd, and L. Vandenberghe, *Convex optimization*. Cambridge university press, 2004.
[33] M. Nick, R. Cherkaoui, and M. Paolone, "Optimal allocation of dispersed energy storage systems in active distribution networks for energy balance and grid support," *IEEE Transactions on Power Systems*, vol. 29, no. 5, 2014.
[34] N. Leemput, F. Geth, J. Van Roy, P. Olivella-Rosell, J. Driesen, and A. Sumper, "MV and LV residential grid impact of combined slow and fast charging of electric vehicles," *Energies*, vol. 8, no. 3, 2015.
[35] Spöttle, M., Jörling, K., Schimmel, M., Staats, M., Grizzel L., Jerram, L., Drier, W., Gartner, J., "Research for TRAN committee - charging infrastructure for electric road vehicles," European Parliament, Policy Department for Structural and Cohesion Policies, Brussels, Tech. Rep., 2018.
[36] Chris Nelder and Emily Rogers, "Reducing EV charging infrastructure costs," Rocky Mountain Institute, Tech. Rep., 2019.
[37] "Schneider EVlink G4 smart charging station - EVB1A22P4ERI," accessed: 2021-08. [Online]. Available: https://bit.ly/3AVUWSO
[38] CIGRE' Task Force C6.04.02, "Benchmark systems for network integration of renewable and distributed energy resources," CIGRE International Council on large electric systems, Tech. Rep., July 2009.
[39] R. Gupta, F. Sossan, and M. Paolone, "Countrywide pv hosting capacity and energy storage requirements for distribution networks: The case of switzerland," *Applied Energy*, vol. 281, p. 116010, 2021.